Jurnal Polimesin
Department of Mechanical Engineering
State Polytechnic of Lhokseumawe
http://e-jurnal.pnl.ac.id/polimesin
e-ISSN : 2549-1999 No. : 3 Month : Ju
p-ISSN : 1693-5462 Volume : 23 Year : 2025

Processing dates: received on 2025-05-09, reviewed on 2025-06-23, accepted on 2025-06-27 and online availability on 2025-06-30

Study on the impact of natural graphite amount and dispersion on the electrical performance of PET/graphite composites

Agus Edy Pramono[1], Anissa Puspa Dewi[1,*], Tatun Hayatun Nufus[1], Nanik Indayaningsih[2]
[1]Magister Program in Applied Manufacturing Technology Engineering, State Polytechnic of Jakarta, Depok 16425, Indonesia
[2]Research Centre for Physics-National Research and Innovation Agency, Banten 15310, Indonesia
*Corresponding Author: anissapuspadewi.tm23@stu.pnj.ac.id

Abstract

Polymer composites have experienced rapid development in recent decades due to their ability to integrate mechanical, thermal, and electrical properties tailored for specific applications. One of the major challenges in polymer development is improving electrical conductivity, as most polymers are inherently insulating. To address this, various conductive fillers such as carbon black, graphite, carbon nanotubes, and graphene have been utilized. This study investigates the effect of natural graphite loading on the electrical conductivity, microstructure, and porosity of virgin Polyethylene Terephthalate (PET) composites. Composites containing 10%, 20%, and 30% graphite by weight were fabricated using the hot compaction method. Morphological analysis via Scanning Electron Microscopy (SEM) revealed that higher graphite content enhances filler connectivity, with the formation of conductive pathways beginning at 20% and a continuous network forming at 30%, despite some agglomeration and weak interfacial bonding. Density measurements and porosity analysis indicated that increasing graphite content leads to greater porosity, with the 30% composite reaching 19.68%. Electrical conductivity increased significantly with increasing graphite loading, exhibiting a transition from insulating to conductive behavior. The percolation threshold was identified at approximately 13.2 wt%, with conductivity rising from 0.00347 S/m at 10 wt% to 6.97 S/m at 30 wt%, consistent with classical percolation theory. These findings demonstrate that natural graphite is an effective conductive filler for PET-based composites and that its content must be optimized to balance conductivity with structural integrity.

Keywords:
PET-based composites; electrical conductivity; hot compaction

1 Introduction

Polyethylene terephthalate (PET) is a thermoplastic material that finds extensive use across industries owing to its favorable mechanical characteristics, low weight, resistance to corrosion, and cost-effective manufacturing process [1], [2]. Despite these advantages, PET exhibits intrinsic insulating properties that limit its applications in fields requiring electrical or thermal conductivity. To overcome this limitation, conductive additives such as graphite are introduced to improve both electrical and thermal conductivity. Polymer Matrix Composites (PMCs) have undergone rapid development in recent decades owing to their tunable mechanical, thermal, and electrical properties, which can be tailored to suit specific applications [3]. A major challenge in advancing PMCs lies in enhancing the electrical conductivity of inherently insulating polymers. To this end, numerous conductive fillers have been explored, ranging from conventional Carbon Black (CB) to advanced nanomaterials such as Carbon Nanotubes (CNTs) and Graphene Nanoplatelets (GNPs) [4]-[6].

Among these, natural graphite has emerged as a promising filler due to its combination of high thermal stability, excellent electrical conductivity, and availability in scalable forms such as flakes or powders. Geologically formed from high-carbon metamorphic rocks under high pressure and temperature, natural graphite is an allotrope of carbon composed of loosely bonded graphene layers held by van der Waals forces. This structure not only facilitates easy processing but also contributes to enhanced conductivity and mechanical reinforcement when incorporated into a polymer matrix. Its broad applicability includes use as battery electrodes, lubricants, conductive materials, and Electromagnetic Interference (EMI) shielding agents. Compared to nano-fillers such as graphene and CNTs, natural graphite provides a more economical and industrially feasible alternative [7], [8].

While microscale fillers have traditionally been employed to enhance the electrical and mechanical characteristics of polymers, they typically require high filler loadings, which can compromise the material's mechanical strength and ease of processing. In contrast, nanoscale fillers are capable of significantly boosting thermal, electrical, and mechanical properties even at low concentrations, and they also offer additional benefits such as improved flame resistance [9], [10]. However, the incorporation of nanofillers introduces challenges like weak interfacial bonding, non-uniform distribution, and particle agglomeration, often making advanced surface treatment or functionalization necessary to achieve a well-dispersed and stable composite structure [11].

The effectiveness of PET–graphite composites strongly depends on the percolation threshold, which refers to the minimum graphite content required to form a continuous conductive network within the matrix [12]. This threshold is influenced by filler morphology, particle size, aspect ratio, and the quality of dispersion in the polymer matrix [13]. To achieve good dispersion and optimal percolation, three methods are used, which are solution mixing, in situ polymerization, and melt mixing. Among these, melt mixing is considered more environmentally friendly and industrially viable, as it avoids the use of solvents and enables large-scale production [14], [15]. Several studies have shown that melt mixing PET with graphite can enhance both electrical and thermal properties without compromising mechanical integrity [16], [17]. However, the process must be carefully optimized to prevent graphite agglomeration, which can deteriorate the composite's conductive performance. Although numerous studies have investigated conductive polymer composites, research specifically exploring the use of natural graphite as a filler in PET-based composites remains limited. In particular, further investigation is needed to characterize the electrical and thermal conductivity of PET–graphite composites and to analyze the percolation threshold. Therefore, this study aims to develop PET–natural graphite composites and evaluate the effect of graphite content on their electrical conductivity.

2 Materials and experimental methods

2.1 Materials and composite preparation

The composite was formulated using virgin PET and natural graphite powder. The PET matrix was derived from Ramapet N1 food-grade pellets (WWRC Indonesia), ground to a mesh size #30. This copolymer has an intrinsic viscosity of 0.80 ± 0.02 dl/g, a melting point of 247 ± 2 °C, a crystalline density of 1.40 g/cm³, and a minimum crystallinity of 50%, with a moisture content below 0.2%, minimizing thermal degradation during processing [18]. Natural graphite, supplied by *Badan Riset dan Inovasi Nasional* (BRIN), was used as the conductive filler in ready-to-use powder form. The graphite has a particle size corresponding to mesh 300,

which facilitates uniform distribution and potential formation of conductive networks at lower filler loadings. It has a density of 2.26 g/cm³, a shear modulus of 2.3 GN/m², and a Young's modulus of 11.3 TN/m². Its high sublimation point (3727–3742 °C) ensures excellent thermal stability, while its low surface energy (1.2 × 10^{-5} J/cm²) promotes good dispersion within the polymer matrix [19], [20]. The PET–Graphite composites were manually mixed without pre-treatment at three weight ratios to observe the effect of graphite loading on electrical performance [21], [22], [23]. The composition details are summarized in Table 1.

Table 1. Composition of PET–graphite composites

Specimen Code	Natural Graphite (%wt)	Virgin PET (%wt)
G1-9VPET	10%	90%
G2-8VPET	20%	80%
G3-7VPET	30%	70%

This stepwise variation was intended to evaluate the influence of graphite concentration on the electrical conductivity of the PET-based composite materials.

2.2 Sample fabrication

The PET–Graphite composites were fabricated using a hot compaction method. Virgin PET powder (Ramapet N1) was blended manually with natural graphite powder at specific weight ratios of 90:10, 80:20, and 70:30 (%wt) until the filler was evenly dispersed throughout the polymer matrix. Graphite filler concentrations of 10%, 20%, and 30% were selected to systematically evaluate the influence of loading level on the composite's electrical performance. This stepwise formulation is commonly employed to identify the percolation threshold and to optimize the trade-off between enhanced conductivity and material processability. Approximately 9 cm³ of the resulting mixture was placed into a steel mold that had been preheated to 100 °C. Compaction was performed in two consecutive stages using a hot compaction press. First, the material was compressed at 100 bar to initiate particle rearrangement. The mold was then briefly opened to release entrapped air, followed by a second compaction at the same pressure to improve densification. The temperature subsequently increased stepwise to 150 °C and 185 °C, each held for 30 minutes, and finally to 210 °C for 60 minutes under steady pressure. After processing, the composites were cooled to room temperature by pouring water over the mold before demolding. The overall fabrication process, including mixing and compaction stages, is illustrated in Fig. 1 to provide a visual representation of the workflow and ensure reproducibility.

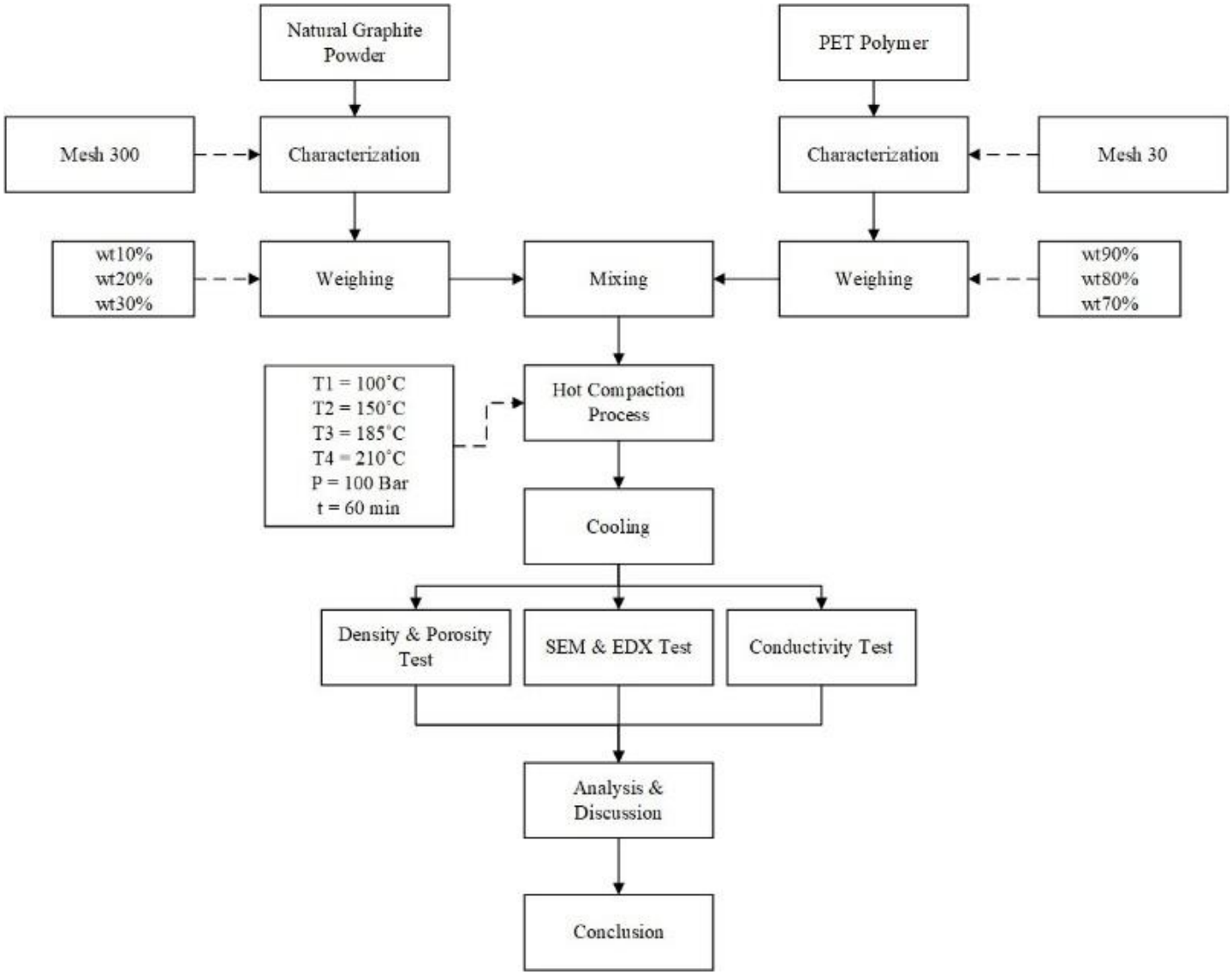

Fig. 1. Fabrication flows of PET-graphite composite

2.3 Characterization techniques

2.3.1 Density measurement

Density measurements were performed following the ASTM D792 standard using the water displacement method. The sample's weight was recorded in both air and submerged in water at room temperature, allowing for precise calculation of its specific gravity. To ensure consistency and repeatability of the results, each measurement was conducted in triplicate (three repetitions per sample). This method is widely adopted in polymer composite research due to its simplicity and precision [24], [25], [26].

2.3.2 Microstructural analysis

Microstructural examination of the PET–Graphite composites was performed at BRIN using a Hitachi SU3500 Scanning Electron Microscope (Japan). Both Secondary Electron (SE) and Backscattered Electron (BSE) modes were employed at varying magnifications (500×, 1000×, 2000×, and 5000×) to assess the

dispersion of graphite particles and the interfacial bonding between filler and matrix. To further investigate the crystalline structure and material phases, X-Ray Diffraction (XRD) analysis was conducted using a TORONTECH TT-EDXPRT X-ray Fluorescence Analyzer (Canada) [27].

2.3.3 Electrical conductivity test

Electrical conductivity measurements were carried out by ASTM D4496 using the four-point probe technique. The experiments utilized a Keithley SourceMeter® 2450 (AS), conducted at the Physics Laboratory of BRIN, Indonesia. A current ranging from –0.1 A to 0.1 A was applied during testing, with the probe holder's resistance maintained at 0.000937 Ω. This configuration allowed for the precise determination of the bulk electrical conductivity of the composite specimens [28].

3 Results and discussion

3.1 Density characteristics of PET-graphite composite

Experimental density measurements of the composite samples were performed using the Archimedes method, as specified in ASTM D792. The method involved weighing the dry sample (in air), the saturated sample (after soaking in water), and the submerged weight (while fully immersed in water). Due to the low density of some samples, a metal sinker with known mass and volume was attached to keep them fully submerged during measurement. This ensured minimal error in determining the buoyant force, which is critical for accurate density estimation in porous or lightweight composites. To evaluate the integrity of the composite fabrication, the measured experimental densities were compared with theoretical predictions calculated using the rule of mixtures. Theoretical density values were obtained by incorporating the volume fractions and known material densities of PET and graphite, as presented in the relevant Eq. (1).

$$\rho\ theoritical = (f\ vol\ VPET \times \rho\ VPET) + (f\ vol\ Graphite \times \rho\ Graphite) \quad (1)$$

On the other hand, the experimental density was evaluated using a formula derived from Archimedes' principle, as shown in Eq. (2).

$$\rho\ experimental = \frac{W_{Dry}}{W_{Saturated\ Air} - W_{Saturated\ Water}} \quad (2)$$

As presented in Table 2, theoretical density exhibited an increasing trend with the incorporation of graphite, which can be attributed to the inherently higher density of graphite relative to PET.

Table 2. Theoretical volume fractions and theoretical densities of PET–graphite composites

Specimen	f vol VPET	f vol Graphite	ρ theoretical (g/cm³)
G1-9VPET	0.9356	0.0644	1.4556
G2-8VPET	0.8664	0.1336	1.5154
G3-7VPET	0.7904	0.2096	1.5812

The measured densities for all samples were lower than their theoretical values shown in Table 3, indicating the presence of voids or porosity within the material due to incomplete compaction or trapped air during the fabrication process. Porosity was calculated based on the difference between theoretical and experimental density using Eq. (3).

Table 3. Experimental measurements and density values of PET–graphite composites

Specimen	Dry Weight (g)	Saturated Air (g)	Saturated Water (g)	ρ experimental (g/cm³)
G1-9VPET	1.92	1.93	0.35	1.21
G2-8VPET	2.07	2.09	0.44	1.26
G3-7VPET	2.46	2.47	0.53	1.27

$$Porosity\ (\%) = \frac{\rho_{theoritical} - \rho_{experimental}}{\rho_{theoritical}} \times 100\% \quad (3)$$

Applying this equation, the porosity values for the G1-9VPET, G2-8VPET, and G3-7VPET specimens were calculated to be approximately 16.86%, 16.82%, and 19.68%, respectively. These values suggest that increasing the graphite content does not linearly reduce porosity, despite graphite's higher density. The highest porosity was observed in the G3-7VPET sample, which contained the most graphite.

As graphite content increased, porosity slightly increased, particularly in G3-7VPET, which reached 19.68% as shown in Table 4 and Fig. 2. This suggests that higher filler content may hinder proper consolidation of the composite, causing higher internal void volume. Similar findings have been reported in various studies, reinforcing this observation.

Table 4. Porosity values of PET–graphite composites

Specimen	ρ theoretical (g/cm³)	ρ experimental (g/cm³)	Porosity (%)
G1-9VPET	1.4556	1.21	16.86
G2-8VPET	1.5154	1.26	16.85
G3-7VPET	1.5812	1.27	19.68

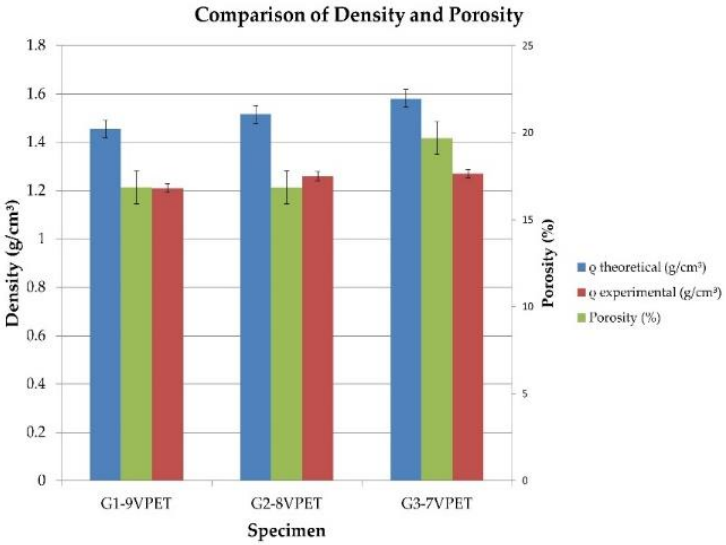

Fig. 2. Comparison of density and porosity of PET-graphite composite

Syahid et al. (2021) found that increasing graphite content in aluminum matrix composites led to a rise in porosity and a decrease in relative density, attributed to poor compaction during powder metallurgy. Likewise, in epoxy-based composites, higher graphite loading resulted in increased internal voids regardless of particle size, indicating that excessive filler content can disrupt matrix continuity [29]. Cerný et al. (2023) further highlighted the critical role of porosity in reducing the mechanical strength of polyurethane composites, emphasizing the need for optimized processing to minimize void formation [30]. Supporting this, Fajri et al. (2022) similarly reported that inadequate filler dispersion and the presence of air pockets during the mixing stage significantly contributed to increased porosity, which in turn adversely affected the composite's physical and mechanical characteristics [31].

3.2 Characterization of microstructure in PET–graphite composite

Figs. 3 (a) to (c) presents surface micrographs of PET–graphite composites with graphite weight fractions of 10%, 20%, and 30%. The samples were synthesized using the hot compaction method with a stepwise temperature increase from 100 to 210 °C, holding each 50-60 °C increment for 30 to 60 minutes. The micrographs reveal that increasing graphite content leads to a more uniform and compact filler distribution.

At 10 wt% graphite, the SEM micrograph (Fig. 4(a)) at ×5000 magnification shows a PET–graphite composite with randomly dispersed graphite particles and several visible voids within the PET

matrix, indicating poor interfacial adhesion and incomplete compaction during the hot-pressing process.

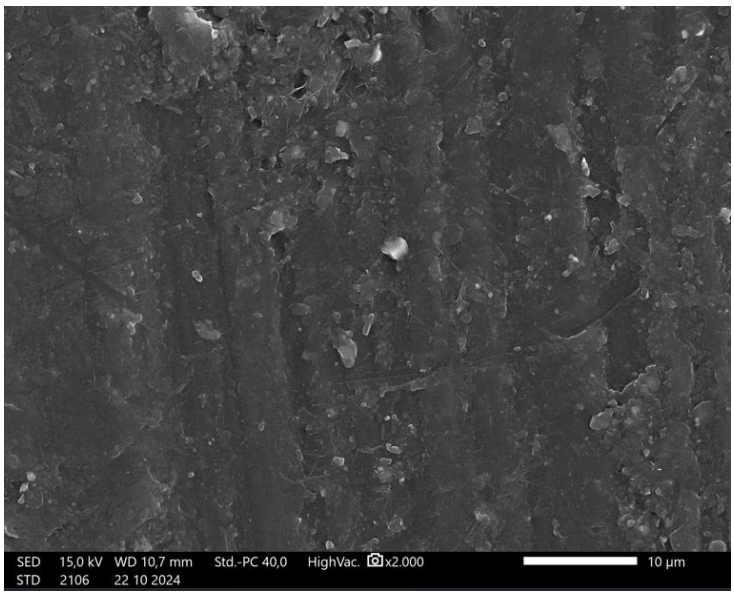

(a)

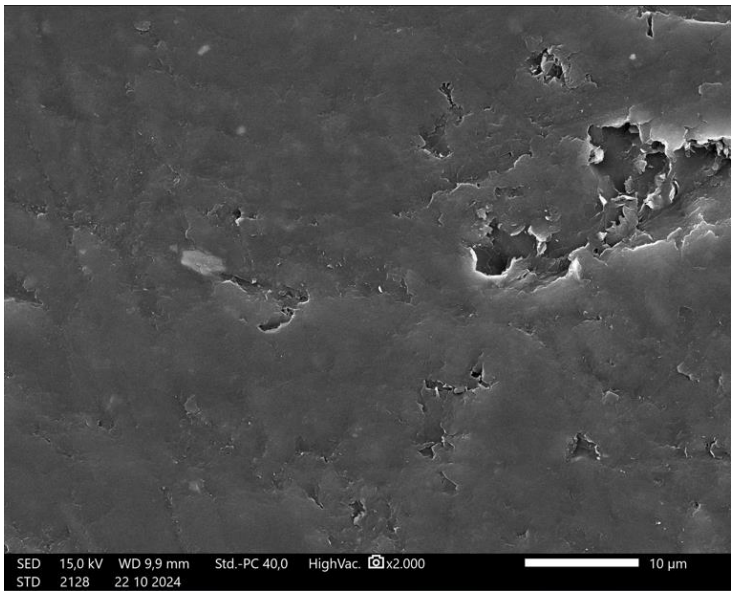

(b)

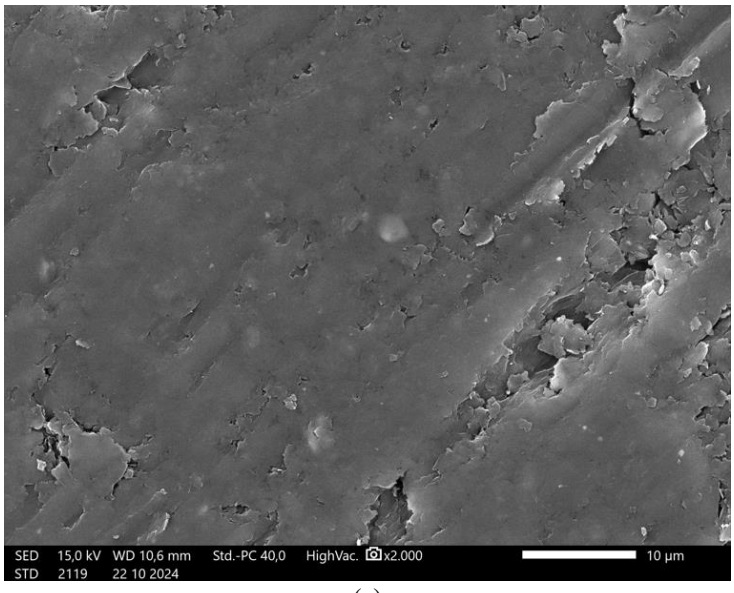

(c)

Fig. 3. Scanning Electron Microscopy (SEM) images of PET/Graphite composites at 2000× magnification for compositions of (a) 10%, (b) 20%, and (c) 30% graphite

The graphite fillers appear isolated, with no continuous conductive network formed, suggesting that the composition is below the percolation threshold. Some agglomerated regions and bright spots are also observed, which are identified as impurities. This is supported by the EDX spectrum, which confirms the presence of major elements such as carbon and oxygen (corresponding to the PET and graphite components) alongside minor traces of silicon, calcium, iron, and chlorine, likely originating from raw materials or environmental contamination.

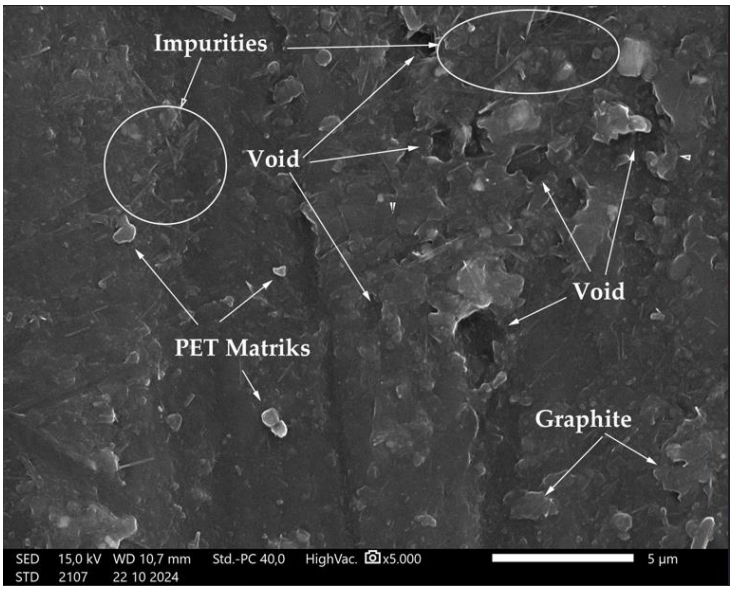

(a)

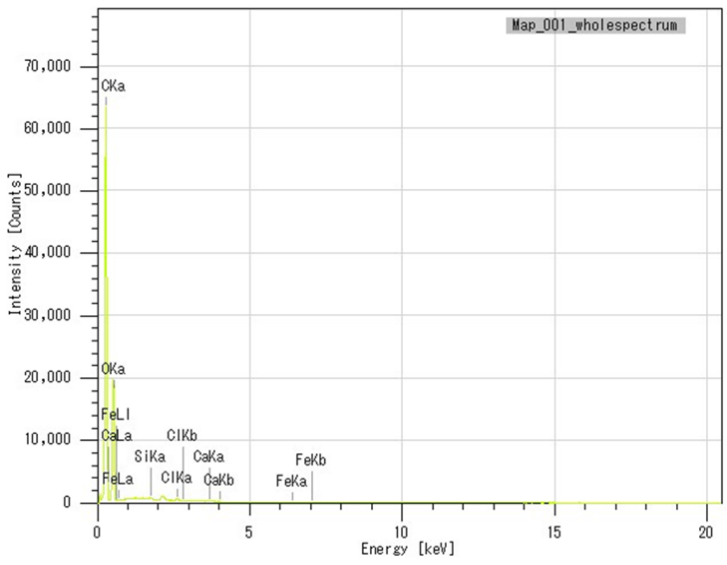

(b)

Fig. 4. (a) SEM micrograph of PET–graphite composite with 10 wt% graphite at ×5000 magnification, and (b) corresponding EDX spectrum

As shown in Fig. 5(b), the SEM image of the composite with 20% graphite reveals the initial formation of conductive pathways between graphite particles, indicating improved filler connectivity within the PET matrix. Graphite particles begin to establish contact, suggesting the development of an electrical network. However, several voids are still present in the matrix, likely resulting from trapped gas or insufficient compaction during processing. Additionally, agglomerated filler regions can be observed, indicating that the dispersion of graphite is not entirely uniform.

In Fig. 5(b), corresponding to the 30% graphite composition, the SEM micrograph exhibits a more interconnected graphite network with layered structures that support continuous conductive pathways. Despite the occurrence of slight agglomeration (likely due to the higher concentration exceeding the optimal dispersion limit), this condition appears to enhance electrical conductivity. Nonetheless, certain graphite particles appear to be separated from the polymer matrix, suggesting insufficient interfacial adhesion between the filler and the PET.

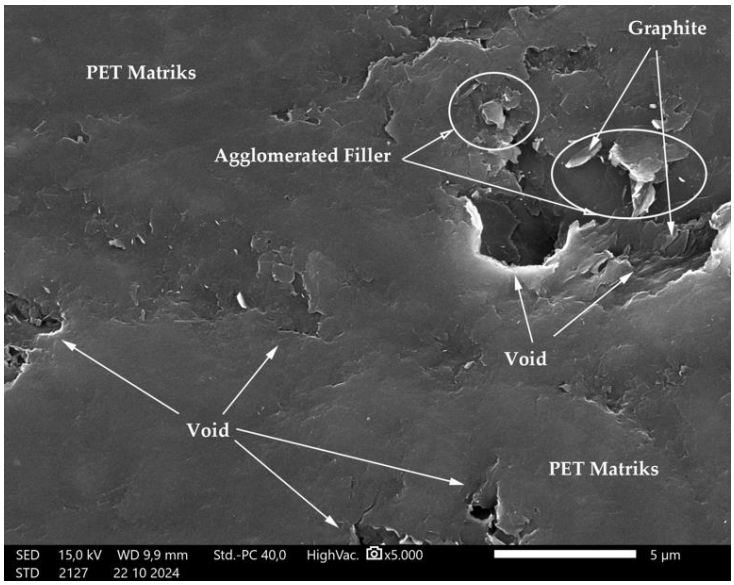

(a)

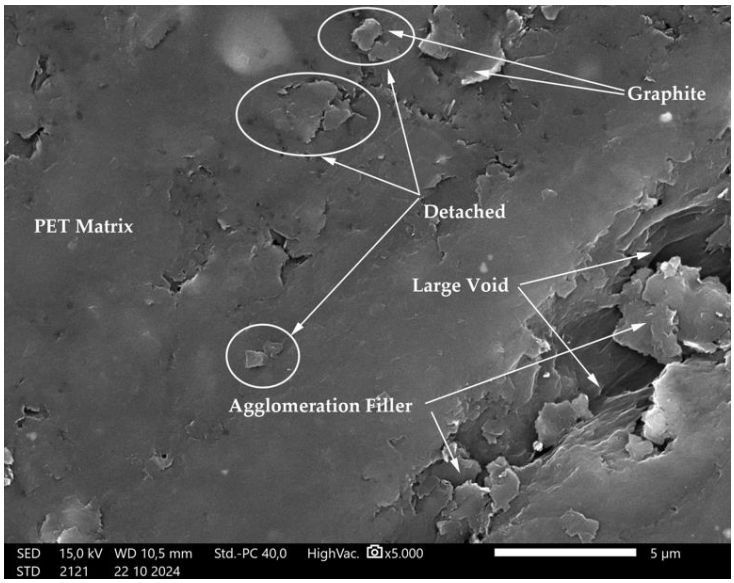

(b)

Fig. 5. (a) SEM image of PET–graphite composite containing 20 wt% graphite captured at 5000× magnification, and (b) SEM image of PET–graphite composite with 30 wt% graphite observed at 5000× magnification

In addition, the occurrence of larger voids becomes more evident at this filler concentration. These voids are likely to increase overall porosity, potentially compromising the composite's mechanical strength and thermal stability [32], [33].

3.3 Evaluation of electrical conductivity of PET–graphite composite

The electrical conductivity (**σ**) of the PET–graphite composites was measured at ambient temperature to investigate how varying graphite content influences the material's conductive properties. Measurements were performed using the four-point probe technique, ensuring high accuracy and reliability in determining σ values for each specimen. In this study, three different graphite loadings 10, 20, and 30 wt%, were selected to examine the percolation behavior and conductivity enhancement in the composite system. The results are presented in Table 5.

Table 5. Electric conductivity values of PET–graphite composites

Specimen	Graphite (wt%)	Electric Conductivity σ (S/m)	R^2 Value
G1-9VPET	10	0.00347	0.99677
G2-8VPET	20	0.04586	0.99862
G3-7VPET	30	6.96506	0.99997

As shown in Table 5, there is a marked increase in electrical conductivity with higher graphite content, suggesting a shift from insulating to conductive behavior, which can be attributed to the development of conductive pathways within the polymer matrix. The percolation threshold was experimentally determined to be approximately 13.2 wt%, which is consistent with previous findings in similar composite systems. Below this threshold, graphite particles remain insufficiently connected, leading to low conductivity. Once this threshold is exceeded, a dramatic rise in conductivity occurs as interconnected conductive networks form throughout the matrix. Fig. 6 presents a log-log graph depicting the relationship between electrical conductivity and the adjusted graphite content ($\Phi - \Phi_c$), where Φ_c represents the percolation threshold at 13.2 wt%. The data exhibit excellent agreement with the power-law relationship (Eq. (4)) [34], [35].

$$\sigma = \sigma_0(\Phi - \Phi_{c)}^{\ t} \quad (4)$$

Where σ_0 is the scaling factor, Φ is the graphite weight fraction, Φ_c is 13.2 wt% is the percolation threshold, and t is the critical exponent associated with the formation dynamics of conductive networks.

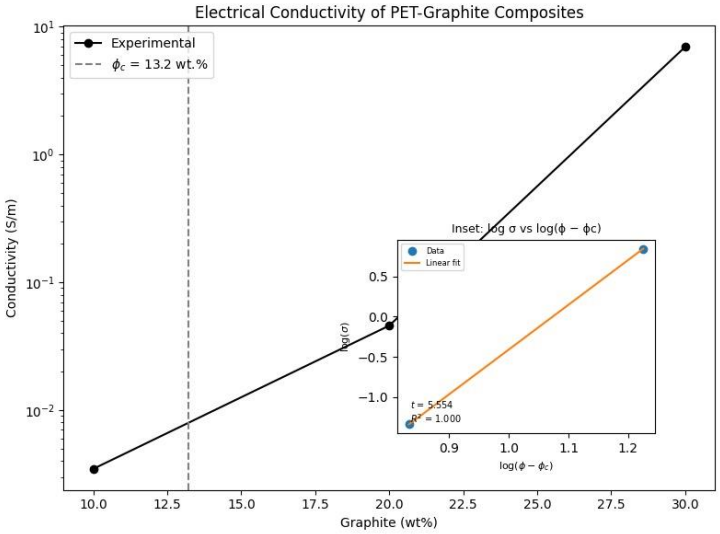

Fig. 6. Percolation threshold graph of electrical conductivity in PET–graphite composites

Linear regression analysis of the log-transformed conductivity data yielded a critical exponent of approximately 0.39 with a correlation coefficient exceeding 0.99, indicating strong agreement with classical percolation theory. This low critical exponent suggests gradual network formation, likely influenced by uniform graphite dispersion, particle shape, and size distribution within the PET matrix. A continuous conductive network begins to emerge as the graphite content approaches the percolation threshold of approximately 13.2 wt%. Below this threshold, graphite particles remain isolated, resulting in poor conductivity (e.g., ~0.003 S/m at 10 wt%) shown in Fig. 6. Slightly above the threshold, at 20 wt%, conductivity increases over tenfold (~0.046 S/m), indicating the onset of conductive path formation. At 30 wt%, conductivity rises sharply to ~7 S/m, reflecting a well-developed conductive network that enables efficient electron transport. These findings demonstrate that tuning the graphite concentration near the percolation threshold allows for precise control of the composite's electrical performance, which is particularly valuable for applications such as sensors and EMI shielding [36]. To further strengthen the interpretation of this conductivity spike, particularly at 30 wt% graphite, SEM micrographs provide critical support. As illustrated in Fig. 5(b), the SEM image at 30 wt% graphite shows a dense and well-connected network of graphite particles distributed throughout the PET matrix, with minimal voids and enhanced interparticle contact. This microstructural observation confirms the establishment of a continuous conductive path that enables efficient electron transport.

Compared to previous studies, this work exhibits a lower percolation threshold and significantly higher conductivity. Alshammari et al. (2019) reported a percolation threshold between 14–15 wt% in PET/graphite micro-composites, with maximum

conductivity of only ~0.0016 S/m, suitable mainly for antistatic applications [37]. Similarly, Chaudhry et al. (2020) found that HDPE composites with 40 wt% graphite nanoplatelets achieved a conductivity of just 3.3×10^{-5} S/cm. In contrast, the present study achieves far superior conductivity at lower filler loadings [38]. Additionally, Tu et al. (2017) reported that electrical percolation in HDPE/PP composites was achieved at 3 wt% for thermally reduced graphene oxide (TRG) and 7 wt% for surfactant-exfoliated graphene (SEG), highlighting the influence of filler type [39]. Graphene's two-dimensional structure enables earlier and more efficient network formation, often resulting in higher conductivity than graphite-based systems [40], [41].

4 Conclusions

This study aimed to investigate the effect of graphite content on the electrical conductivity and microstructural characteristics of PET–graphite composites. The results demonstrate that increasing graphite loading significantly enhances electrical conductivity, with a percolation threshold identified at approximately 13.2 wt%. Beyond this threshold, the composite transitions from insulation to conductive behavior, attributed to the formation of interconnected conductive networks within the PET matrix. The SEM analysis confirmed that at 30 wt% graphite, a well-connected and layered graphite microstructure is established, which facilitates efficient charge transport. However, the increase in graphite content also introduces greater porosity, with the highest porosity recorded at 19.68%, potentially compromising the mechanical integrity and thermal stability of the material. In conclusion, the research successfully meets its objectives by demonstrating the correlation between graphite loading, electrical performance, and microstructural development in PET-based composites. These findings underscore the importance of optimizing filler content to achieve a functional balance between electrical conductivity and structural reliability for potential applications in antistatic materials, sensors, and EMI shielding.

References

[1] R. Nisticò, "Polyethylene terephthalate (PET) in the packaging industry," Oct. 01, 2020, *Elsevier Ltd*. doi: 10.1016/j.polymertesting.2020.106707.

[2] Y. Srithep *et al.*, "Processing and characterization of recycled poly(ethylene terephthalate) blends with chain extenders, thermoplastic elastomer, and/or poly(butylene adipate-co-terephthalate)," *Polym Eng Sci*, vol. 51, no. 6, pp. 1023–1032, 2011, doi: 10.1002/pen.21916.

[3] S. Thalib, S. Zakaria, C. H. Azhari, I. Muhammad, and H. Usman, "Jurnal Polimesin," vol. 23, no. 2, pp. 203–208, 2025.

[4] M. R. Karim, C. J. Lee, and M. S. Lee, "Synthesis and characterization of conducting polythiophene/carbon nanotubes composites," *J Polym Sci A Polym Chem*, vol. 44, no. 18, pp. 5283–5290, Sep. 2006, doi: 10.1002/pola.21640.

[5] X. Sun, H. Sun, H. Li, and H. Peng, "Developing polymer composite materials: Carbon nanotubes or graphene?," Oct. 04, 2013. doi: 10.1002/adma.201301926.

[6] L. S. Schadler, L. C. Brinson, and W. G. Sawyer, "Polymer Nanocomposites: A Small Part of the Story," *Nanocomposite Materials Overview*, 2007.

[7] M. Simón, A. Benítez, A. Caballero, J. Morales, and O. Vargas, "Untreated natural graphite as a graphene source for high-performance Li-Ion batteries," *Batteries*, vol. 4, no. 1, Mar. 2018, doi: 10.3390/batteries4010013.

[8] B. A. Alshammari, A. N. Wilkinson, and G. Almutairi, "Electrical, Thermal, and Morphological Properties of Poly(ethylene terephthalate)-Graphite Nanoplatelets Nanocomposites," *Int J Polym Sci*, vol. 2017, 2017, doi: 10.1155/2017/6758127.

[9] W. Yang *et al.*, "Functionalized Carbon Nanotubes with Phosphorus- and Nitrogen-Containing Agents: Effective Reinforcer for Thermal, Mechanical, and Flame-Retardant Properties of Polystyrene Nanocomposites," *ACS Appl Mater Interfaces*, vol. 8, no. 39, pp. 26266–26274, Oct. 2016, doi: 10.1021/acsami.6b06864.

[10] S. E. Zhu *et al.*, "Comparative studies on thermal, mechanical, and flame retardant properties of PBT nanocomposites via different oxidation state phosphorus-containing agents modified amino-CNTs," *Nanomaterials*, vol. 8, no. 2, Feb. 2018, doi: 10.3390/nano8020070.

[11] N. G. Sahoo, S. Rana, J. W. Cho, L. Li, and S. H. Chan, "Polymer nanocomposites based on functionalized carbon nanotubes," Jul. 2010. doi: 10.1016/j.progpolymsci.2010.03.002.

[12] B. A. Alshammari, F. S. Al-Mubaddel, M. R. Karim, M. Hossain, A. S. Al-Mutairi, and A. N. Wilkinson, "Addition of graphite filler to enhance electrical, morphological, thermal, and mechanical properties in poly (ethylene terephthalate): Experimental characterization and material modeling," *Polymers (Basel)*, vol. 11, no. 9, 2019, doi: 10.3390/polym11091411.

[13] C. O. Blattmann and S. E. Pratsinis, "Nanoparticle filler content and shape in polymer nanocomposites," Jan. 10, 2019, *Hosokawa Powder Technology Foundation*. doi: 10.14356/kona.2019015.

[14] R. F. Brandenburg, C. M. Lepienski, D. Becker, and L. A. F. Coelho, "Influence of mixing methods on the properties of high density polyethylene nanocomposites with different carbon nanoparticles," *Revista Materia*, vol. 22, no. 4, 2017, doi: 10.1590/S1517-707620170004.0222.

[15] M. Rahaman, A. Aldalbahi, and P. Bhagabati, "Preparation/Processing of Polymer–Carbon Composites by Different Techniques," 2019, pp. 99–124. doi: 10.1007/978-981-13-2688-2_3.

[16] E. N. N. A. Ansar, M. N. Biutty, K. S. Kim, S. Yoo, P. H. Huh, and S. Il Yoo, "Sustainable Polyamide Composites Reinforced with Nanocellulose via Melt Mixing Process," Oct. 01, 2024, *Multidisciplinary Digital Publishing Institute (MDPI)*. doi: 10.3390/jcs8100419.

[17] J. H. Kim, J. S. Hong, A. Ishigami, T. Kurose, H. Ito, and K. H. Ahn, "Effect of melt-compounding protocol on self-aggregation and percolation in a ternary composite," *Polymers (Basel)*, vol. 12, no. 12, pp. 1–17, Dec. 2020, doi: 10.3390/polym12123041.

[18] "Technical Datasheet RAMAPET N1(S)" [Online]. Available: www.indoramapolymers.eu

[19] A. D. Jara, A. Betemariam, G. Woldetinsae, and J. Y. Kim, "Purification, application and current market trend of natural graphite: A review," Sep. 01, 2019, *China University of Mining and Technology*. doi: 10.1016/j.ijmst.2019.04.003.

[20] M. Simón, A. Benítez, A. Caballero, J. Morales, and O. Vargas, "Untreated natural graphite as a graphene source for high-performance Li-Ion batteries," *Batteries*, vol. 4, no. 1, Mar. 2018, doi: 10.3390/batteries4010013.

[21] O. A. Alo and I. O. Otunniyi, "Graphite-Filled Polyethylene/Epoxy Blend for High-Conductivity Applications: The Immiscibility Edge," *Polymer-Plastics Technology and Materials*, pp. 105–116, 2020, doi: 10.1080/25740881.2020.1793195.

[22] M. H. A. El Salam, G. M. Elkomy, H. Osman, M. R. Nagy, and F. El-Sayed, "Structure-electrical conductivity of polyvinylidene fluoride/graphite composites," *Journal of Reinforced Plastics and Composites*, vol. 31, no. 20, pp. 1342–1352, Oct. 2012, doi: 10.1177/0731684412459286.

[23] I. Tavman *et al.*, "Effects of conductive graphite filler loading on physical properties of high-density polyethylene composite," *Polym Compos*, vol. 33, no. 7, pp. 1071–1076, Jul. 2012, doi: 10.1002/pc.22230.

[24] A. E. Pramono, S. Ruswanto, and N. Indayaningsih, "Effect of pyrolysis sintering temperature on the electrical current delivery

power of kaolin-carbon composites," *Journal of Ceramic Processing Research*, vol. 23, no. 2, pp. 171–180, 2022, doi: 10.36410/jcpr.2022.23.2.171.
[25] A. E. Pramono, H. Rahman, P. M. Adhi, and N. Indayaningsih, "Controlling the size and carbon composition to determine the electrical conductivity of the kaolin-carbon composite," *Journal of Ceramic Processing Research*, vol. 23, no. 5, pp. 638–646, Oct. 2022, doi: 10.36410/jcpr.2022.23.5.638.
[26] S. A. Agrawal, "Simplified Measurement of Density of Irregular Shaped Composites Material using Archimedes Principle by Mixing Two Fluids Having Different Densities," *International Research Journal of Engineering and Technology*, 2021, [Online]. Available: www.irjet.net
[27] A. Zuhri, A. E. Pramono, I. Setyadi, A. Maksum, and N. Indayaningsih, "Effect of microcarbon particle size and dispersion on the electrical conductivity of LLDPE-carbon composite," 2024. [Online]. Available: www.jart.icat.unam.mx
[28] Y. Yang *et al.*, "High performance carbon-based planar perovskite solar cells by hot-pressing approach," *Solar Energy Materials and Solar Cells*, vol. 210, Jun. 2020, doi: 10.1016/j.solmat.2020.110517.
[29] M. Syahid, A. Hayat, and Aswar, "Effect of Graphite Addition on Aluminum Hybrid Matrix Composite by Powder Metallurgy Method," *Revue des Composites et des Materiaux Avances*, vol. 32, no. 3, pp. 125–132, Jun. 2022, doi: 10.18280/rcma.320303.
[30] M. Černý, J. Petruš, and I. Chamradová, "The Influence of Porosity on Mechanical Properties of PUR-Based Composites: Experimentally Derived Mathematical Approach," *Polymers (Basel)*, vol. 15, no. 8, Apr. 2023, doi: 10.3390/polym15081960.
[31] A. Hasnul Fajri Arsyah, I. Hari Mulyadi, and J. Affi, "Pengaruh Penambahan Filler Al 2 O 3 dan TiO 2 pada Resin Polyester terhadap Sifat Fisik dan Mekanik," *JURNAL Teknik Mesin*, vol. 16, no. 2, pp. 104–110, 2023, [Online]. Available: http://ejournal2.pnp.ac.id/index.php/jtm
[32] M. Mehdikhani, L. Gorbatikh, I. Verpoest, and S. V. Lomov, "Voids in fiber-reinforced polymer composites: A review on their formation, characteristics, and effects on mechanical performance," May 01, 2019, *SAGE Publications Ltd*. doi: 10.1177/0021998318772152.
[33] Z. Liu, Y. Lei, X. Zhang, Z. Kang, and J. Zhang, "Effect Mechanism and Simulation of Voids on Hygrothermal Performances of Composites," *Polymers (Basel)*, vol. 14, no. 5, Mar. 2022, doi: 10.3390/polym14050901.
[34] S. Paszkiewicz *et al.*, "Electrical conductivity of poly(ethylene terephthalate)/expanded graphite nanocomposites prepared by in situ polymerization," *J Polym Sci B Polym Phys*, vol. 50, no. 23, pp. 1645–1652, Dec. 2012, doi: 10.1002/polb.23176.
[35] W. Bauhofer and J. Z. Kovacs, "A review and analysis of electrical percolation in carbon nanotube polymer composites," *Compos Sci Technol*, vol. 69, no. 10, pp. 1486–1498, Aug. 2009, doi: 10.1016/j.compscitech.2008.06.018.
[36] X. Jiang, D. X. Yan, Y. Bao, H. Pang, X. Ji, and Z. M. Li, "Facile, green and affordable strategy for structuring natural graphite/polymer composite with efficient electromagnetic interference shielding," *RSC Adv*, vol. 5, no. 29, pp. 22587–22592, 2015, doi: 10.1039/c4ra11332b.
[37] B. A. Alshammari, F. S. Al-Mubaddel, M. R. Karim, M. Hossain, A. S. Al-Mutairi, and A. N. Wilkinson, "Addition of graphite filler to enhance electrical, morphological, thermal, and mechanical properties in poly (ethylene terephthalate): Experimental characterization and material modeling," *Polymers (Basel)*, vol. 11, no. 9, 2019, doi: 10.3390/polym11091411.
[38] A. U. Chaudhry, S. P. Lonkar, R. G. Chudhary, A. Mabrouk, and A. A. Abdala, "Thermal, electrical, and mechanical properties of highly filled HDPE/graphite nanoplatelets composites," in *Materials Today: Proceedings*, Elsevier Ltd, 2019, pp. 704–708. doi: 10.1016/j.matpr.2020.04.168.
[39] C. Tu, K. Nagata, and S. Yan, "Morphology and electrical conductivity of polyethylene/polypropylene blend filled with thermally reduced graphene oxide and surfactant exfoliated graphene," *Polym Compos*, vol. 38, no. 10, pp. 2098–2105, Oct. 2017, doi: 10.1002/pc.23782.
[40] A. Tarhini and A. R. Tehrani-Bagha, "Advances in Preparation Methods and Conductivity Properties of Graphene-based Polymer Composites," Dec. 01, 2023, *Springer Nature*. doi: 10.1007/s10443-023-10145-5.
[41] C. Tu, K. Nagata, and S. Yan, "Dependence of Electrical Conductivity on Phase Morphology for Graphene Selectively Located at the Interface of Polypropylene/Polyethylene Composites," *Nanomaterials*, vol. 12, no. 3, Feb. 2022, doi: 10.3390/nano12030509.